

# Computational Exploration of $\pi$ -4f Magnetic Interaction in the Excited-State Heterometallic Triple-Decker Porphyrinoid Lanthanide Complex

Anas Santria,<sup>1,2</sup> and Naoto Ishikawa<sup>1</sup>

<sup>1</sup>Graduate School of Science, The University of Osaka

<sup>2</sup>Research Center for Chemistry, National Research and Innovation Agency

## 1. Introduction

In our previous reports, we established the existence and fundamental characteristics of magnetic interactions in mono- and bis-phthalocyanine/porphyrin lanthanide(III) complexes. [1] These interactions occur between the total angular momentum of the localized 4f system (**J**) and the orbital angular momentum generated from the cyclic  $\pi$ -conjugated system (**L**), henceforth referred to as the **J-L** interaction. Through combined MCD experiments and *ab initio* calculations, we observed that these interactions can exhibit either ferromagnetic- or antiferromagnetic-type, depending on the lanthanide ion (e.g., Ferromagnetic for Tb, Er, Yb; antiferromagnetic for Dy). The studies have mapped how **J-L** manifests in single- and double-decker structures and how ligand identity and coordination geometry affect the sign and magnitude of these interactions. [2] Building on this foundation, this work shifts its focus to a heterometallic, triple-decker phthalocyanine formulated as  $\text{Pc}_3\text{LnY}$  (where  $\text{Ln}^{3+}$  and  $\text{Y}^{3+}$  occupy metal sites). By introducing a diamagnetic  $\text{Y}^{3+}$  center in place of one of the metal sites, a system is created in which (a)  $\text{Ln}^{3+}$  experiences an altered coordination environment without magnetic disruption from the second metal ion and (b) the overall ligand field and  $\pi$ -electron delocalization framework are modified relative to the homometallic analogue. In this way, the Tb-Y system serves as an important bridge between our double-decker model and the more extensive ligand stack.

Here, our investigation focused on heterometallic triple-decker phthalocyanine complexes containing

terbium(III) and yttrium(III) to gain initial insights into photoinduced **J-L** interactions. By pairing  $\text{Tb}^{3+}$  with a diamagnetic  $\text{Y}^{3+}$  center in a three-layer phthalocyanine stack, we constructed a model system where the **J-L** character can be examined without the interference of additional 4f orbital contributions, and where the ligand field and  $\pi$ -electron topology evolve across the three phthalocyanine rings.

## 2. Computational Methods

The structure of  $\text{TAP}_3\text{Y}_2$  (TAP = Tetraazaporphyrin (basic structure of phthalocyanine); Y = yttrium) was constructed using the Avogadro program. The geometry optimization process was carried out using Gaussian 16, revision C.01, at the B3LYP level of theory with Grimme D3 dispersion and Becke-Johnson damping. The basis set 6-31G(d,p) was utilized for C, H, and N atoms, while LANL2DZ basis sets were employed for the Y ion.

Multiconfigurational calculations were carried out using OpenMolcas version 24.10. ANO-RCC basis sets were applied to all atoms. The computational procedure involved a complete/restricted active space self-consistent field (CASSCF/RASSCF) calculation, followed by restricted active space state interaction (RASSI) and Single\_Aniso modules analyses.

## 3. Results and Discussion

In this study, we extend our investigation of the magnetic interaction between the angular momentum generated by the localized 4f system, particularly the total angular momentum (**J**) of Ln(III) and the orbital angular momentum (**L**) of  $\pi$ -conjugated ligands, to the

triple-decker phthalocyaninato complex  $\text{TAP}_3\text{TbY}$ . This system is fascinating due to its extended  $\pi$  system, sandwich-type coordination, and the axial asymmetry introduced by the inclusion of the diamagnetic Y(III) ion in the middle layer. For comparison, we refer to the previously studied double-decker  $\text{Pc}_2\text{Tb}^-$  complex, which serves as a benchmark for evaluating the effect of sandwich layer expansion on the strength and properties of **J-L** interaction.

### 3.1 The Ground State Structure of $\text{TAP}_3\text{TbY}$

To establish a foundation for studying **J-L** interactions in the excited state of  $\text{TAP}_3\text{TbY}$ , we first determined its ground multiplet structure using CASSCF with an active space that contains seven 4f orbitals housing eight electrons, referred to as CAS(8,7). The geometric structure was derived from the optimized  $\text{TAP}_3\text{Y}_2$  structure by substituting one Y with a Tb ion. In this calculation, seven roots of configuration interaction (CI) were employed, leading to forty-nine distinct electron configurations in the terbium 4f manifold. Notably, these seven 4f orbitals are positioned between occupied  $\pi$  orbitals (directly below) and unoccupied  $\pi$  orbitals (directly above), ensuring the 4f manifold remains well separated from the  $\pi$  ligand framework. This orbital arrangement serves as the basis for all subsequent analyses.

When examining the ground multiplet states of  $\text{TAP}_3\text{TbY}$ , we found a closely isolated  $|\pm 6\rangle$  doublet at essentially zero energy (separated by only  $0.004\text{ cm}^{-1}$ ), composed of equal contributions of 50%  $|+6\rangle$  and 50%  $|-6\rangle$ . This nearly pure  $J_z = \pm 6$  character reflects the predominantly axial crystal field, albeit slightly weaker than its  $\text{Pc}_2\text{Tb}^-$ . The first excited doublet appears at  $290.7\text{ cm}^{-1}$  and already shows a 50/50 mixture of  $|+5\rangle$  and  $|-5\rangle$ , indicating the onset of  $J_z$  mixing at lower energies compared to  $\text{Pc}_2\text{Tb}^-$  (where the corresponding pure  $|\pm 5\rangle$  state is located at  $337.1\text{ cm}^{-1}$ ). At  $471.9\text{ cm}^{-1}$ , the next state consists of about 41%  $|\pm 4\rangle$  and 18%  $|0\rangle$ , while the nearest level at  $492.6$

$\text{cm}^{-1}$  is once again dominated (50%) by  $|\pm 4\rangle$ , indicating that the purity of  $|\pm 4\rangle$  is only partially restored. Above this, at roughly  $536\text{ cm}^{-1}$ , there are two nearly degenerate multiplets where  $J_z = \pm 3$  and  $\pm 1$  are mixed in equal parts (25% each), and at  $543.8\text{ cm}^{-1}$ , a balanced (50/50)  $|\pm 2\rangle$  doublet appears. At  $594.9\text{ cm}^{-1}$ , the first singlet with predominantly  $|0\rangle$  character (82%) appears, accompanied by a minor  $|\pm 4\rangle$  contribution, and two additional mixed multiplets near  $626.7\text{ cm}^{-1}$  complete the low-lying multiplet.

Compared to  $\text{Pc}_2\text{Tb}^-$ , where each low-lying multiplet remains essentially a pure  $|\pm J_z\rangle$  doublet up to nearly  $800\text{ cm}^{-1}$ , the  $\text{TAP}_3\text{TbY}$  complex exhibits a smaller energy gap between  $|\pm 6\rangle$  and its first excited multiplet, along with a significant mixing of the  $J_z$  components at intermediate energies. This difference indicates that the triple-decker TAP ligand field, while still largely axial, introduces a low-symmetry perturbation that reduces the crystal field splitting.

Having established the energy positions and wave function composition of the ground multiplet sublevels, we can now proceed to incorporate  $\pi$  orbital interactions into the excited state analysis. In the next section, we will build on these ground state energies, specifically the zero-field splitting of the  $|\pm 6\rangle$  doublet, to explore how excitation into the  $\pi$  manifold modifies the **J-L** coupling. By including three highest occupied  $\pi$  orbitals (HOMO, HOMO-1, and HOMO-2) and six lowest unoccupied  $\pi$  orbitals (LUMO, LUMO+1, LUMO+2, LUMO+3, LUMO+4, and LUMO+5) in addition to the 4f orbitals, we will evaluate the extent to which  $\pi$  electron delocalization influences the terbium **J-L** interactions in the  $\text{TAP}_3\text{TbY}$  excited state.

### 3.2 Excited States of $\text{TAP}_3\text{TbY}$

With the ground-state multiplet structure established, we next direct our attention to the  $\pi$ - $\pi^*$  excited states of  $\text{TAP}_3\text{TbY}$ , aiming to quantify how the orbital angular momentum generated by the ligand (**L**) interacts with the total angular momentum of the 4f

system (**J**) upon  $\pi$ - $\pi^*$  excitation. To capture the relevant 4f and  $\pi$ -orbital characteristics, the active space was expanded from CAS(8,7) to CAS(14,16). In this CAS(14,16), the seven 4f orbitals of Tb(III) are positioned between the three highest occupied  $\pi$  orbitals and the six lowest unoccupied  $\pi^*$  orbitals of the TAP<sub>3</sub> structure. By applying a total of 388 CI roots, we obtained the total low-lying energy of the spin-orbit (SO) states as 2716.

Table 1. Selected transition energy and angular momenta of TAP<sub>3</sub>TbY extracted from CASSCF/RASSI/SINGLE\_ANISO calculations.

Doublet	Energy (cm <sup>-1</sup> )	Osc. Strength (initial doublet → final doublet)	L <sub>z</sub>	S <sub>z</sub>	J <sub>z</sub>   =  L <sub>z</sub> + S <sub>z</sub>
1	0		3.00	3.00	6.00
294	29311	0.04 (1→294)	6.01	3.00	9.01
295	29313	0.04 (1→295)	0.03	3.00	2.97
347	31266	0.06 (1→347)	4.95	3.00	7.95
348	31273	0.06 (1→348)	1.10	2.98	4.08
595	39005	0.06 (1→595)	4.41	3.00	7.41
596	39014	0.06 (1→596)	1.57	3.00	4.57

The analysis of the oscillator strength was conducted to identify the SO states that contribute to the Q-band absorption of TAP<sub>3</sub>TbY. Several transitions from the two nearly degenerate lowest SO states (designated as doublet 1) to the higher energy, nearly degenerate excited SO states were found to exhibit significant oscillator strengths. Notable transitions include those to SO states 588 and 589 (doublet 294, 29311 cm<sup>-1</sup>), 590 and 591 (doublet 295, 29313 cm<sup>-1</sup>), 694 and 695 (doublet 347, 31266 cm<sup>-1</sup>), 696 and 697 (doublet 348, 31273 cm<sup>-1</sup>), 1190 and 1191 (doublet 595, 39005 cm<sup>-1</sup>), and 1191 and 1193 (doublet 596, 39014 cm<sup>-1</sup>), as summarized in Table 1.

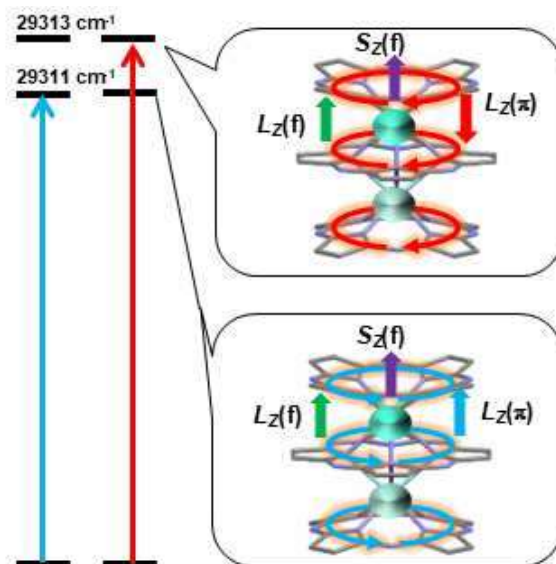


Figure 1: Schematic **J-L** interaction in the excited states of TAP<sub>3</sub>TbY.

Further analysis was conducted on the values of  $|L_z|$  and  $|S_z|$  for all selected doublets. In the ground doublet (doublet 1),  $|L_z| = 3.00$  and  $|S_z| = 3.00$  combine to yield  $|J_z| = 6.00$ , which aligns well with the pure  $J_z = \pm 6$  projection for Tb<sup>3+</sup>. Because  $L_z$  in the ground doublet is generated solely by the 4f system, this  $L_z$  is referred to as  $L_z(4f)$ . Upon transitioning to doublet 294,  $|L_z|$  increases to approximately 6.01 while  $|S_z|$  remains at 3.00, resulting in  $|J_z| = 9.02$ . In other words, the  $\pi \rightarrow \pi^*$  transition contributes about three units of orbital angular momentum ( $\Delta L_z$  about +3) parallel to  $L_z(4f)$ , as illustrated in Figure 1. In the higher excited doublet, doublet 295 (the pair of doublet 294), the  $|L_z|$  decreases to approximately 0.03 while  $|S_z|$  remains at 3.00, yielding  $|J_z| = 2.97$ . Here,  $\Delta L_z$  about -3 indicates that the  $\pi$ -derived orbital momentum is oriented antiparallel to  $L_z(4f)$ . Since the parallel arrangement is more stable than the antiparallel arrangement, the interaction favors a ferromagnetic-type interaction. For other pairs of excited doublets, such as doublets 347 and 348, as well as doublets 595 and 596, the situation is similar, with a parallel arrangement occurring in each lower excited doublet:  $\Delta L_z$  about 1.9 and 1.6 for the pairs 347/348 and 595/596. Regarding

the magnitude of the interaction, similar to our previous reports [1,3],  $\Delta_{JL}$  is defined as the half-energy separation between the lower and higher excited states. Consequently, we obtained the  $\Delta_{JL}$  values of about 1  $\text{cm}^{-1}$ , 3.5  $\text{cm}^{-1}$ , and 9.5  $\text{cm}^{-1}$  for the pairs 294/295, 347/348, and 595/596, respectively.

### 3.3 Diamagnetic Analogue Comparison for Orbital Angular Momentum

To verify that the  $\pi$  system is indeed the source of additional angular momentum, we compared the results with those of the isostructural diamagnetic analogue,  $\text{TAP}_3\text{Y}_2$ . In this calculation, we included six electrons in the three highest  $\pi$  orbitals (HOMO, HOMO-1, HOMO-2) to the active space 1, and six lowest unoccupied  $\pi$  orbitals (LUMO, LUMO+1, LUMO+2, LUMO+3, LUMO+4, and LUMO+5) to the active space 3. This resulted in several excited doublet states with significant  $|Lz|$  values, such as 2.34, 2.97, and 2.66, for the excited states at 19895  $\text{cm}^{-1}$  (doublet 2), 28754  $\text{cm}^{-1}$  (doublet 4), and 33473  $\text{cm}^{-1}$  (doublet 6), respectively. Here, the observed  $Lz$  values are generated solely from the  $\pi$  ligand system, and thus, the observed  $Lz$  is referred to as  $Lz(\pi)$ . Among these, the transition to doublet 4 (28754  $\text{cm}^{-1}$ ) has an oscillator strength of 0.08 and  $|Lz|$  of 2.97. This value closely aligns with the  $\Delta Lz$  observed in the  $\text{TAP}_3\text{TbY}$  transitions, especially for the pair doublets 294/295, confirming that the additional angular momentum originates from the ligand  $\pi$  system. This direct comparison validates our interpretation of the **J–L** interaction as a coupling between the angular momentum generated by the 4f system and the angular momentum produced by the cyclic  $\pi$  system of the porphyrinoid ligand.

## 4. Conclusion

In conclusion, this study provides a comprehensive computational exploration of the  $\pi$ –4f magnetic interactions in the excited states of heterometallic

triple-decker porphyrinoid lanthanide complexes. By comparing the diamagnetic  $\text{TAP}_3\text{Y}_2$  complex with the paramagnetic  $\text{TAP}_3\text{TbY}$  system, we clarified how ligand-centered  $\pi$ – $\pi^*$  excitations can interact with the 4f orbitals of a single Tb(III) ion through **J–L** coupling. Multireference *ab initio* calculations demonstrate that the excited-state splitting correlates with the  $\pi$  orbital angular momentum, affirming the crucial role of the ligand electronic structure in influencing the 4f excited-state magnetism. These findings highlight the potential of porphyrinoid-based platforms to engineer excited-state magnetic interactions, offering new insights for the rational design of photoresponsive lanthanide complexes for molecular magnetism and quantum information applications

## Acknowledgements

All calculations have been done using supercomputer system SQUID at the Cybermedia Center (currently:D3 Center), The University of Osaka.

## References

- (1) (a) K. Kizaki, et al., *Chem. Commun.*, **53**, 6168-6171, (2017); (b) T. Fukuda, et al., *Chem. Eur. J.*, **23**, 16357-16363, (2017). (c) A. Santria, and N. Ishikawa, *Inorg. Chem.*, **59**, 14326-14336, (2020); (d) K. Kizaki, et al., *Inorg. Chem.*, **60**, 2037-2044, (2021); (e) A. Santria, and N. Ishikawa, *Inorg. Chem.*, **60**, 14418-14425, (2021); (f) L.C. Adi, et al., *Dalton Trans.*, **51**, 6186-6196, (2022); (g) K. Kizaki, et al., *Inorg. Chem. Front.*, **10**, 915-925, (2023); (h) A. Santria, サイバーメディア HPC ジャーナル, 2023, 13, p. 45- 49; (i) L. C. Adi, et al., *Dalton Trans.*, **53**, 628-639, (2024).
- (2) A. Santria, and N. Ishikawa, サイバーメディア HPC ジャーナル, 2024, 14, p. 47- 52;
- (3) A. Santria, and N. Ishikawa, *J. Phys. Chem. A*, **128**, 6722-6728, (2024)